Applied Numerical Modeling in Geomechanics – 2020 – Billaux, Hazzard, Nelson & Schöpfer (eds.) Paper: 17-03

Optimized stability assessment of tunneling stress redistribution under geological lateral pressures

W.C. Chang & W.J. Shiu
Geotechnical Engineering Research Center, SINOTECH Engineering Consultants, Inc., Taipei, Taiwan, ROC

1 INTRODUCTION

Localized stability in a rock medium during tunneling may depend on stress variation in the surrounding materials, which is correlated with the critical stress states of the rock medium. Due to the fact that the analytical or empirical methods sometimes cannot account for all factors influencing tunnel stability, numerical simulations of stability assessment are widely developed over many years. Many researchers investigate tunnel stability by using certain quantized indices of safety factor and have conducted numerical modelling analyses. Dhawan et al. (2002) evaluated the stability of underground openings when extensive realistic input data was available for nonhomogeneous rock masses. Chen & Tseng (2010) simulated horseshoe tunnels and found that the most critical excavation cycles with significant stability variation always happened during the two cycles before and after monitoring stations. Kulatilake et al. (2013) simulated the stress conditions around a tunnel located under high in-situ stress conditions within a coal rock mass in China with a numerical *3DEC* model, and the comparison between the distribution of failure zones and stress field can be achieved via the optimum stability within tunnel shape and support pattern. Soren et al. (2014) proposed a numerical *FLAC* modeling technique to be used to predict the stress-strain behavior of pit slopes and evaluate the stability analysis of open pit slopes. Chen & Chang (2017) discovered that tunnel roof stability can be improved by stereographic projection of minimum principal stress direction within the three-dimensional principal stress distribution. Therefore, A *FLAC3D* (Itasca 2017) model is used in this study to establish the mechanism of overall three-dimensional stress variations under different lateral pressure conditions (K=0.5,1,2) during excavating. The purpose of this study is to provide a safety of factor calculation based on a normalized deviatoric plane of Mohr-Coulomb's envelope, which can demonstrate the complicated spatial three-dimensional stress path of every tunneling round, and contribute to optimized stability assessment in the application of practical tunnel construction.

2 DESIGN AND ANALYSIS

In traditional tunnel construction, the stability can be evaluated quickly by using the Mohr-Coulomb failure criterion. However, the shortcoming of Mohr's circle is that it considers just the maximum and minimum principal stress for factor of safety (FS) calculation, and also creates inconvenience when analyzing many Mohr's circles.

However, the aforementioned factor of safety sometimes overestimates the stability by only taking the maximum and minimum principal stress (σ_1, σ_3) into consideration during tunneling. The ignored intermediate principal stress σ_2 may sometimes induce excavation risk, especially under contrasting lateral pressures. In this study, the tunnel stability can be evaluated as accurately as possible using the new modified factor of safety calculation by the redistribution of stress path.

In order to illustrate more clearly the redistribution of stress path, the specific deviatoric plane of every tunneling round will be normalized. Puzrin (2011) mentioned that stress space can be shown as the selected symbol $(\xi、\rho_\theta、\theta)$ within the represent yield and failure functions from Equation (1) to Equation (3). Equation (4) gives the relation between $(,\sigma_2,\sigma_3)$ and (ξ,ρ_θ,θ).

$$\xi=\frac{(\sigma_1+\sigma_2+\sigma_3)}{\sqrt{3}} \tag{1}$$

$$\rho_\theta=\sqrt{2J_2} \tag{2}$$

$$\cos3\theta=\frac{3\sqrt{3}}{2}\frac{J_3}{{J_2}^{1.5}} \tag{3}$$

$$\begin{Bmatrix}\sigma_1\\ \sigma_2\\ \sigma_3\end{Bmatrix}=\frac{1}{\sqrt{3}}\begin{Bmatrix}\xi\\ \xi\\ \xi\end{Bmatrix}+\sqrt{\frac{2}{3}}\rho\begin{Bmatrix}\cos\theta\\ \cos\left(\theta-\frac{2}{3}\pi\right)\\ \cos\left(\theta-\frac{2}{3}\pi\right)\end{Bmatrix}\text{ , where } 0\le\theta\le\frac{\pi}{3} \tag{4}$$

And Mohr-Coulomb failure criterion can be expressed as Equation (5)

$$f(\xi、\rho、\theta)=\sqrt{2}\xi\sin\phi+\sqrt{3}\rho\sin\left(\theta+\frac{\pi}{3}\right)+\rho\cos\left(\theta+\frac{\pi}{3}\right)-\sqrt{6}\cos\phi=0 \tag{5}$$

Where the conversion formulas are listed from Equation (6) to Equation (10)

$$J_2=\frac{1}{3}({I_1}^2-3I_2) \tag{6}$$

$$J_3=\frac{1}{27}(2{I_1}^3-9I_1I_2+27I_3) \tag{7}$$

$$I_1=(\sigma_1+\sigma_2+\sigma_3) \tag{8}$$

$$I_2=(\sigma_1\sigma_2+\sigma_2\sigma_3+\sigma_3\sigma_1) \tag{9}$$

$$I_3=(\sigma_1\sigma_2\sigma_3) \tag{10}$$

Thence, the spatial principal stress variations during tunneling can be expressed by Mohr-Coulomb failure criterion in 3D principal stress space with their own corresponding deviatoric planes, which depends on the ξ value as in Figs 1a. The major contribution of this study is the unique normalized algorithm, which can integrate every tunneling round into a common deviatoric plane by dividing their own intercept $\rho_t(\xi)$, eliminating the divergence of hexagon from the deviatoric plane of different stress states. To realize the influences of intermediate principal stress, the derivation of dividing axes on the normalized deviatoric plane such as $({\sigma_1}^N,{\sigma_3}^N)$ and the third axis (angular bisector) are calculated within the stress σ_2 bellow. Moreover, the angular bisector is added as the third axis to form two areas (Zones I, Zone II) to analyze the tunneling mechanism of stress path variations as Figs 1b. This study will also take the excavation of the tunnel roof for instance and discuss the stress path of critical rounds under different lateral pressures as shown in Figure 1c. Finally, the new optimized factor of safety $(\mathrm{FS}=\rho_{\theta,max}/\rho_{\theta,})$ can be defined for the purpose of tunnel roof stability in Figure 1d.

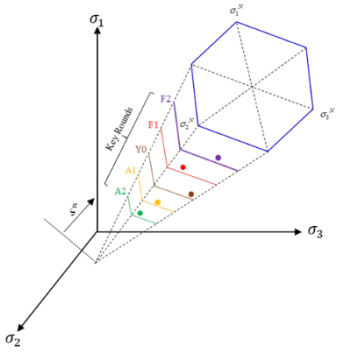

(a) Excavating Stress variation in 3D stress space

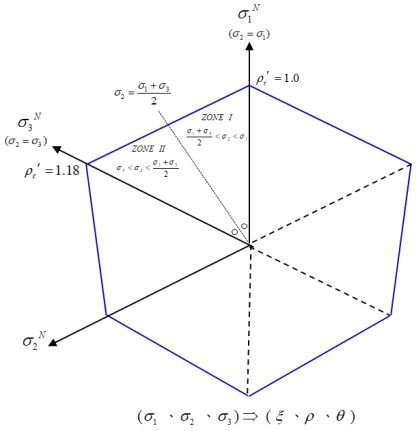

(b) Stress points on spatial deviatoric plane

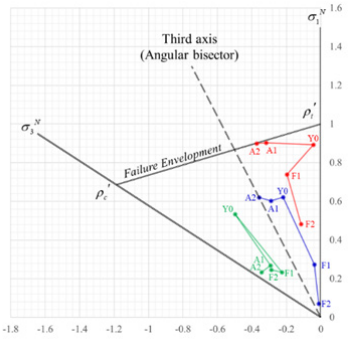

(c) Tunneling stresses variations in space

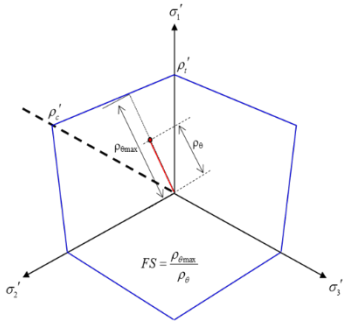

(d) New factor of safety on normalized deviatoric plane

Figure 1. Optimized Stability Algorithm with normalized deviatoric plane.

To sum up, these stress projections and stress path on normalized deviatoric plane are useful in understanding the characteristics of overall tunnel stability. The stability evaluation in this study is considered with the intermediate principal stress. The factor of safety without considering the intermediate principal stress σ_2 can be replaced as in equation (11).

$$\mathrm{FS} = \frac{2c_f * cos\phi - (\sigma_1 + \sigma_3) * sin\phi}{|(\sigma_1 - \sigma_3)|} \tag{11}$$

Although the existence of intermediate principal stress may cause the some influence of safety evaluation, this study still found that (FS) and (FS′) will have the same evaluating result while stress variation points are located in the third axis (angular bisector) $\sigma_2 = (\sigma_1 + \sigma_3)/2$ as in equation (12).

$$\mathrm{FS}' = \frac{\rho_{max}}{\rho_\theta} = \frac{\sqrt{2} * cos\phi - \frac{\sigma_1 + \sigma_3}{\sqrt{2}} * sin\phi}{\left|\frac{\sigma_1 - \sigma_3}{\sqrt{2}}\right|} = \frac{2c_f * cos\phi - (\sigma_1 + \sigma_3) * sin\phi}{|(\sigma_1 - \sigma_3)|} = \mathrm{FS} \tag{12}$$

3 RESULTS AND DISCUSSION

The numerical software *FLAC3D* is adopted to generate the tunnel model for recording the three-dimensional principal stress variations at tunnel roof during excavating as Fig 2. By using the aforementioned algorithm, those important tunneling rounds (F2, F1, Y0, A1, A2) are also summarized the divergences between (FS) and (FS′) for assessing tunnel stability. In general, Eq. 12 predicts a more conservative factor of safety, comparing to the one obtained by Eq. 11.

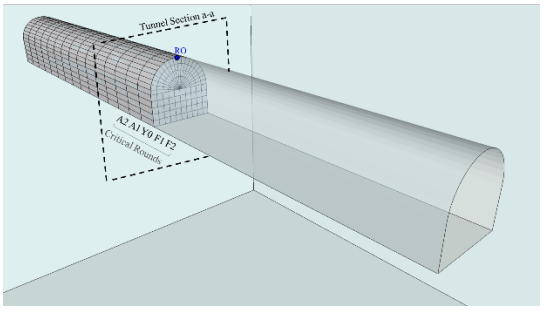

(a) Monitoring station RO at tunnel roof

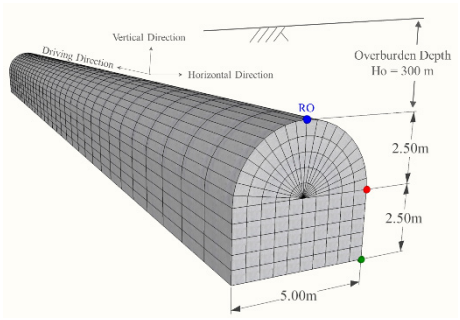

(b) Horseshoes tunnel section size

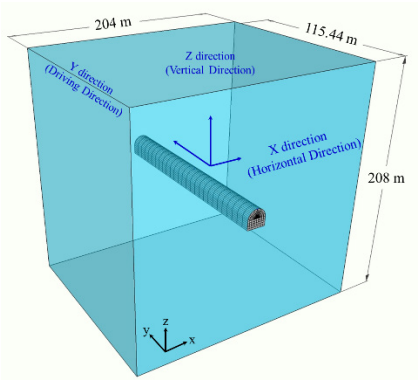

(c) Coordinate and Boundary of 3D tunnel model

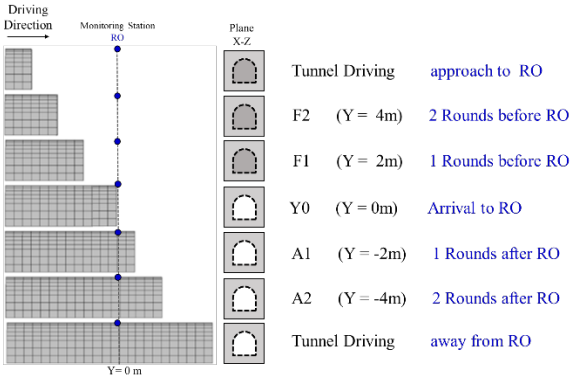

(d) The important tunneling rounds

Figure 2. The establishment of 3D numerical tunnel model.

Furthermore, the different lateral pressures $(K = 0.5, 1.0, 2.0)$ have significant deviation effects based on the existence of the intermediate principal stress, which may be an important contribution from modification (FS') in this study, especially for highly lateral pressure. The distance between the failure envelope and the initial position $(K = 2.0)$ is the closest among all lateral conditions, resulting in much more risk than the lower lateral pressure one as shown in Figure 3. The comparison of safety assessment under the three lateral pressures are listed in Table 3.

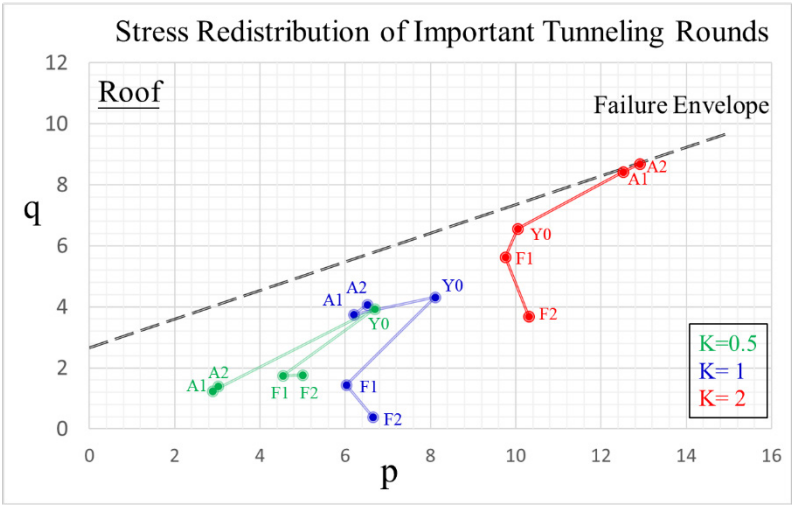

Figure 3. Stress redistribution of important tunneling rounds under different lateral pressures

Table 3. Comparison of Safety Assessment at tunnel roof under different K values.

Lateral Pressures		K=0.5		K=1		K=2	
Critical Rounds \	Factor of Safety	FS	FS′	FS	FS′	FS	FS′
F2		4.41	3.08	26.9	13.6	2.94	1.95
F1		4.27	2.90	6.30	3.54	1.53	1.26
Y0		1.89	1.50	1.93	1.47	1.23	1.10
A1		5.23	3.41	1.91	1.47	1.02	1.01
A2		4.59	3.11	1.75	1.40	1.00	1.00

4 CONCLUSIONS

The conclusions of this study are summarized as follows:

Three-dimensional safety evaluation of rock stresses in this study includes analyzing magnitudes of the principal stresses, calculating the corresponding projection points within failure envelopes, and assessing the factor of safety via a special normalized algorithm on tunnel roof stability. While the conventional safety assessment (FS) can produce the tunnel engineering expediently, the method will not always yield the most robust and reliable tunnel engineering design. The normalized stability algorithm of 3D safety evaluation (FS′) accounts for all principal stresses influences, which is an enhancement over and above the shortcomings of original assessment method. This enhancement will affect the stability outcome during the excavating process.

In view of the optimized evaluation algorithm in the study, the traditional method of Mohr's circle application, which omits the influence of intermediate principal stress, is more suitable for preliminary and rapid estimation. Although the optimized algorithm including three-dimensional principal stress is more complicated in assessing stability, the comprehensive consideration of 3D principal stress variation on the stability can be fully mentioned in the application of practical field construction.

REFERENCES

Chen, C.N. & Huang, W.Y. 2007. Investigation of tunnel stress path during face advancement. *Journal of Mechanics*, Vol. 23, pp. 451-458.

Chen, C.N. & Tseng, C.T. 2010. 2D tunneling chart from redistributed 3D principal stress path. *Tunnelling and Underground Space Technology*, Vol. 25, pp. 305-314.

Chen, C.N. & Chang, W.C. 2017. Directional projection in stereographic representation of three-dimensional stress redistribution during tunnelling. *Tunnelling and Underground Space Technology,* Vol. 70, pp. 309-316.

Eberhardt, E. 2001. Numerical modelling of three-dimension stress rotation ahead of an advancing tunnel face. *International Journal of Rock Mechanics and Mining Sciences,* Vol. 38, pp. 499-518.

Itasca Consulting Group, Inc. 2017. *FLAC3D – Fast Lagrangian Analysis of Continua in 3 Dimensions, Ver. 6.0*. Minneapolis: Itasca.

Galli G., Grimaldi, A. & Leonardi, A. 2004. Three-dimensional modelling of tunnel excavation and lining. *Computers and Geotechnics,* Vol. 31, pp. 171-183.

Ren, G., Smith, J.V., Tang, J.W. & Xie, Y.M. 2005, Underground excavation shape optimization using an evolutionary procedure. *Computers and Geotechnics,* Vol. 32, pp. 122-132.

Clausen, J., Damlilde, L. & Andersen, L. 2006. Efficient return algorithms for associated plasticity with multiple yield planes. *International Journal for Numerical Methods in Engineering,* Vol. 66, pp. 1036-1059.

Dhawan, K.R., Singh, D.N. & Gupta, I.D. 2002. 2D and 3D finite element analysis of underground openings in an in homogeneous rock mass. *International Journal of Rock Mechanics and Mining Sciences and Geomechanics Abstracts,* Vol. 39, pp. 217-227.

Kulatilake, P.H.S.W., Wu, Q., Yu, Z. & Jiang, F. 2013. Investigation of stability of a tunnel in a deepcoal mine in China. *International Journal of Mining Science and Technology,* Vol. 23, pp. 579-589.

Soren, K., Budi, G. & Sen, P. 2014. Stability analysis of open pit slope by finite difference method. *International Journal of Renewable Energy Technology,* Vol. 3, pp. 326-334.

Puzrin, A. 2011. Constitutive Modelling in Geomechanics : Introduction. *Springer Science & Business Media*, pp. 171-183.